01 Apr 2002

A New Layered Iron Fluorophosphates

Amitava Choudhury

Missouri University of Science and Technology, choudhurya@mst.edu

Recommended Citation

A. Choudhury, "A New Layered Iron Fluorophosphates," *Journal of Chemical Sciences*, vol. 114, no. 2, pp. 93-105, Springer India, Apr 2002.

The definitive version is available at https://doi.org/10.1007/BF02704302

Proc. Indian Acad. Sci. (*Chem. Sci.*), Vol. 114, No. 2, April 2002, pp 93–105

A new layered iron fluorophosphate

AMITAVA CHOUDHURY
Chemistry and Physics of Materials Unit, Jawaharlal Nehru Centre for Advanced Scientific Research, Jakkur PO, Bangalore 560 064, India, and Solid State and Structural Chemistry Unit, Indian Institute of Science, Bangalore 560 012, India
e-mail: amitava@jncasr.ac.in

MS received 30 March 2001; revised 26 June 2001

Abstract. A new iron fluorophosphate of the composition, $[C_6N_4H_{21}][Fe_2F_2(HPO_4)_3][H_2PO_4]\cdot 2H_2O$, **I** has been prepared by the hydrothermal route. This compound contains iron fluorophosphate layers and the $H_2PO_4^-$ anions are present in the interlayer space along with the protonated amine and water molecules. The compound crystallizes in the monoclinic space group $P2_1/c$. (a = 13·4422(10) Å, b = 9·7320(10) Å, c = 18·3123(3) Å, β = 92·1480°, V = 2393·92(5) Å^3, Z = 4, M = 719·92, $d_{calc.}$ = 1·997 g cm^{-3}, R_1 = 0·03 and wR_2 = 0·09).

Keywords. Open-framework materials; layered iron phosphate, hydrothermal synthesis.

1. Introduction

Several open-framework transition metal phosphates are known to date[1], those of iron forming a large family[2]. A series of oxy-fluorinated open-framework iron phosphates are also reported[3–5]. Examples of organically templated iron phosphate materials prepared by hydrothermal method, include, one dimensional[6–8], two dimensional[9–17] and three dimensional[14,18–28] structures. We have prepared a new 2-D iron fluorophosphate of the composition, $[C_6N_4H_{21}][Fe_2F_2(HPO_4)_3][H_2PO_4]\cdot 2H_2O$, **I**, under hydrothermal condition. An interesting feature of the compound is that $H_2PO_4^-$ units along with the water molecules are intercalated between the iron fluorophosphate layers.

2. Experimental

The title compound **I** was synthesized under mild hydrothermal conditions starting with a coordination complex of Fe^{3+}, $Fe(acac)_3$ as the source of iron. In a typical synthesis procedure, 0·200 g of $Fe(acac)_3$ was dispersed in 2 ml (2 g) of water. To this, 0·2220 g of H_3PO_4 (85% w/w) was added with constant stirring, followed by the addition of 0·0828 g of *tris*(2-aminoethylamine) (TREN). To this mixture 0·0566 g HF (48% w/w) was added and stirring was continued for another 20 min to obtain a homogenous gel. The final mixture with a molar ratio of $Fe(acac)_3$:$4H_3PO_4$: TREN : 5HF : 200 H_2O was transferred to a 7 ml PTFE-lined acid digestion bomb and heated at 150°C for 40 h. The resultant product contained plate-shaped crystals suitable for single crystal X-ray diffraction in the form of spiked ping-pong balls (as seen under optical microscope), which was

subsequently washed thoroughly with double distilled water and dried at ambient temperature. Compound **I** can be obtained with a wide range of $Fe(acac)_3$ and H_3PO_4 ratios (1 : 3–6) with other conditions remaining the same. $Fe(acac)_3$ was prepared following a reported procedure[29] and rest of the chemicals were obtained from Aldrich and used without further purification. The powder X-ray diffraction (XRD) pattern (figure 1) of the powdered single crystals indicated that the product was a new material, and was consistent with the structure determined by single-crystal X-ray diffraction. A least squares fit of the powder XRD (CuKα) lines of the bulk sample, using the *hkl* indices generated from single crystal X-ray data, gave the following cell: a = 13·4347(1), b = 9·7171(2), c = 18·3107(1) Å and β = 92·1432(1)º, which is in good agreement with that determined by single crystal XRD. Powder data for **I**, $[C_6N_4H_{21}][Fe_2F_2(HPO_4)_3][H_2PO_4]\cdot 2H_2O$, is listed in table 1. The presence of two equivalents of fluorine has been confirmed by chemical analysis (obs. 5%, calc. 5·27%)[30]. Thermogravimetric analysis was carried out (TGA) under nitrogen atmosphere in the range from 25° to 850°C.

A suitable single crystal (0·10 × 0·16 × 0·24 mm) of the title compound was carefully selected under a polarizing microscope and glued to a thin glass fiber with cyanoacrylate (superglue) adhesive. Crystal structure determination by X-ray diffraction was performed on a Siemens Smart-CCD diffractometer equipped with a normal focus, 2·4 kW sealed tube X-ray source (MoKα radiation, λ = 0·71073 Å) operating at 50 kV and 40 mA. A hemisphere of intensity data was collected at room temperature in 1321 frames with ω scans (width of 0.30° and exposure time of 20 s per frame). The final unit cell constants were determined by a least squares fit of 1931 reflections in the range 3° < 2θ < 46·5°. Pertinent experimental details for the structure determinations are presented in table 2. An absorption correction based on symmetry equivalent reflections was applied using SADABS[31] program. Other effects, such as absorption by the glass fiber were simultaneously corrected.

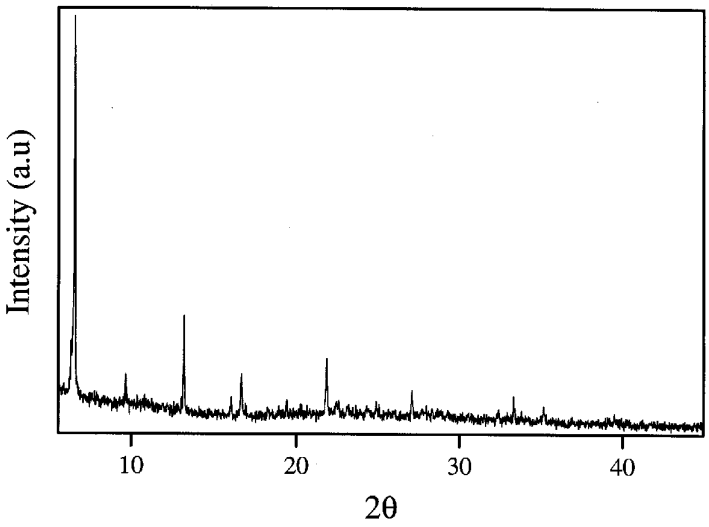

Figure 1. Powder X-ray diffraction pattern for $[C_6N_4H_{21}][Fe_2F_2(HPO_4)_3][H_2PO_4]\cdot 2H_2O$ (**I**).

The structure was solved by direct methods using SHELXS-86[32] and difference Fourier syntheses. The hydrogen positions were initially located in the difference Fourier maps and for the final refinement, the hydrogen atoms were placed geometrically and held in the riding mode. The hydrogens for the water molecules were located and refined isotropically. The last cycles of refinement included atomic positions for all the atoms, anisotropic thermal parameters for all non-hydrogen atoms and isotropic thermal parameters for all the hydrogen atoms. Full-matrix least-squares refinement against $|F^2|$ was carried out using the SHELXTL-PLUS[33] suit of programs. Details of the final refinements are given in table 2. The selected bond distances and bond angles for **I** are given in tables 3 and 4.

3. Results and discussion

The asymmetric unit of **I** (figure 2) contains 36 non-hydrogen atoms, of which 19 atoms belong to the inorganic framework while the rest belong to the guest molecules residing in the inter-lamellar space. The structure of **I** is constructed from the macroanionic inorganic framework layers of $Fe_2F_2(HPO_4)_3^{2-}$, held together by strong hydrogen bonding with an assembly of protonated amine, H_2PO_4 and H_2O. The inorganic framework layer consists of a complex network of vertex-sharing FeF_2O_4, $FeFO_5$ and HPO_4 polyhedra. The connectivity between these polyhedra creates 3, 4 and 8-membered rings within the layer as shown in figure 3. The inorganic layers are stacked along the *a*-axis in the *AAAA* fashion and the interlayer space is occupied by protonated amine, $H_2PO_4^-$ anions and water molecules as shown in figure 4.

Table 1. X-ray powder data for **I** $[C_6N_4H_{21}][Fe_2F_2(HPO_4)_3][H_2PO_4]\cdot 2H_2O$.

h	k	l	$2\theta_{obs}$	$\Delta(2\theta)^a$	d_{calc}	$\Delta(d)^b$	$I_{rel}{}^c$
1	0	0	6·603	0·02	13·426	−0·04	100·0
0	0	2	9·695	0·025	9·146	−0·023	12·4
2	0	0	13·203	0·015	6·713	−0·008	6·3
2	1	0	16·052	0·008	5·524	−0·003	2·6
2	0	2	16·685	0·024	5·321	−0·008	6·4
0	2	0	18·232	−0·019	4·861	0.005	3·6
2	1	2	19·012	−0·001	4·667	0·001	< 1
0	0	4	19·435	0·026	4·573	−0·006	2·9
1	0	−4	20·276	−0·01	4·378	0·002	3·2
3	1	0	21·87	0·008	4·065	−0·001	5·8
2	2	0	22·62	0·037	3·937	−0·006	7·2
2	1	−4	24·906	0·003	3·575	0	6·0
3	2	0	27·1	0·018	3·292	−0·002	5·8
1	3	0	28·337	0·007	3·15	−0·001	3.7
4	2	0	32·425	0·012	2·762	−0·001	2.1
4	2	1	32·922	−0·018	2·719	0·002	2·0
5	0	0	33·348	−0·02	2·685	0·002	< 1
5	0	4	39·53	0·003	2·28	0	1·0
6	1	−4	45·436	−0·007	1·996	0	< 1
6	2	4	49·739	−0·014	1·833	0	< 1
2	1	−10	51·984	−0·013	1·754	0·005	< 1
8	0	2	56·064	−0·005	1·64	0	< 1

[a] $2\theta_{obs.} - 2\theta_{calc.}$; [b] $d_{obs.} - d_{calc.}$; [c] $100 \times I/I_{max}$

Table 2. Crystal data and structure refinement parameters for **I** $[C_6N_4H_{21}][Fe_2F_2(HPO_4)_3][H_2PO_4]\cdot 2H_2O$.

Chemical formula	$Fe_2P_4F_2O_{18}N_4C_6H_{30}$
Space group	$P2_1/c$
T (K)	293
a (Å)	13·4422(10)
b (Å)	9·7320(10)
c (Å)	18·3123(3)
α (deg)	90·0
β (deg)	92·1480(10)
γ (deg)	90·0
Volume (Å^3)	2393·92(5)
Z	4
Formula mass	719·92
ρ_{calc} (gcm^{-3})	1·997
λ (MoKα) Å	0·71073
μ (mm^{-1})	1·583
θ range (°)	1·52–23·29
Total data collected	9785
Index ranges	$-14 \le h \le 11, -10 \le k \le 10, -20 \le l \le 19$
Unique data	3439
Observed data ($I > 2\sigma(I)$)	2901
Absorption correction	SADABS
R_{int} before and after parameter refinement	0·0627 and 0·0355
Max. and min. transmission	1·000000 and 0·675393
Refinement method	Full-matrix least-squares on $\|F^2\|$
R indices [$I > \sigma(I)$]	$R_1 = 0{\cdot}03$, $wR_2 = 0{\cdot}09$
R indices (all data)	$R_1 = 0{\cdot}04$, $wR_2 = 0{\cdot}09^{\#1}$
Goodness of fit (S)	1·09
No. of variables	341
Largest difference map peak and hole eÅ^{-3}	0·645 and −0·730

[1] $w = 1/[\sigma^2(F_O)^2 + (0{\cdot}0541P)^2 + 1{\cdot}2026\text{P}]$, where $P = [F_O{}^2 + 2F_C{}^2]/3$

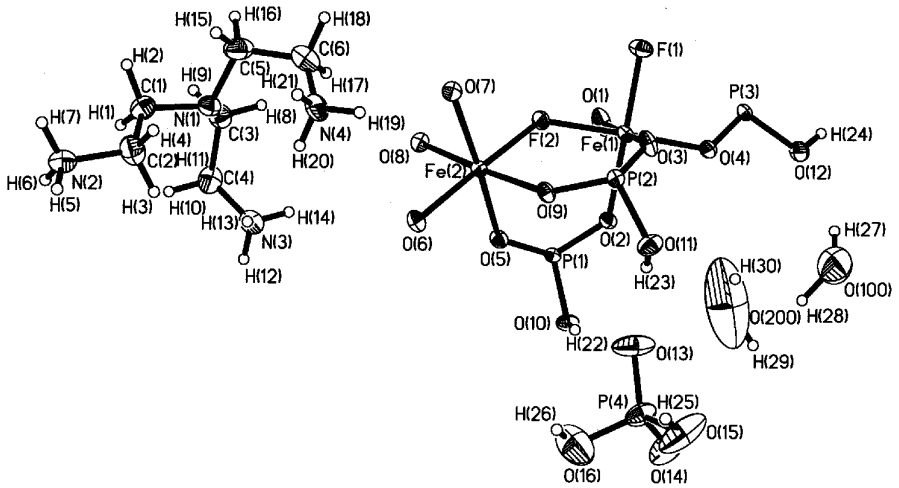

Figure 2. The ORTEP plot of **I** $[C_6N_4H_{21}][Fe_2F_2(HPO_4)_3][H_2PO_4]\cdot 2H_2O$. The asymmetric unit is labelled. Thermal ellipsoids are given at 40% probability.

Table 3. Selected bond distances in **I** $[C_6N_4H_{21}][Fe_2F_2(HPO_4)_3][H_2PO_4]\cdot 2H_2O$.

Moiety	Distance (Å)	Moiety	Distance (Å)
Fe(1)–F(1)	1·915(2)	P(1)–O(2)	1·524(3)
Fe(1)–O(1)	1·953(3)	P(1)–O(10)	1·577(3)
Fe(1)–O(2)	1·972(2)	P(2)–O(9)	1·522(3)
Fe(1)–F(2)	1·977(2)	P(2)–O(8) [#2]	1·523(3)
Fe(1)–O(3)	2·014(3)	P(2)–O(3)	1·524(3)
Fe(1)–O(4)	2·015(2)	P(2)–O(11)	1·574(3)
Fe(2)–F(2)	1·956(2)	P(3)–O(1) [#3]	1·491(3)
Fe(2)–O(5)	1·960(2)	P(3)–O(4)	1·520(3)
Fe(2)–O(6)	1·985(2)	P(3)–O(6) [#4]	1·526(3)
Fe(2)–O(7)	1·989(2)	P(3)–O(12)	1·588(3)
Fe(2)–O(8)	1·998(3)	P(4)–O(13)	1·482(3)
Fe(2)–O(9)	2·049(3)	P(4)–O(14)	1·495(3)
P(1)–O(5)	1·514(3)	P(4)–O(15)	1·538(3)
P(1)–O(7) [#1]	1·518(3)	P(4)–O(16)	1·554(4)
Organic moiety			
N(1)–C(5)	1·457(5)	C(1)–C(2)	1·502(6)
N(1)–C(3)	1·463(5)	C(4)–N(3)	1·475(6)
N(1)–C(1)	1·470(5)	C(5)–C(6)	1·490(7)
		C(6)–N(4)	1·486(6)

Symmetry transformations used to generate equivalent atoms: [#1] $-x, y - 1/2, -z + 3/2$; [#2] $-x, y + 1/2, -z + 3/2$; [#3] $-x, -y, -z + 1$; [#4] $x, -y + 1/2, z - 1/2$

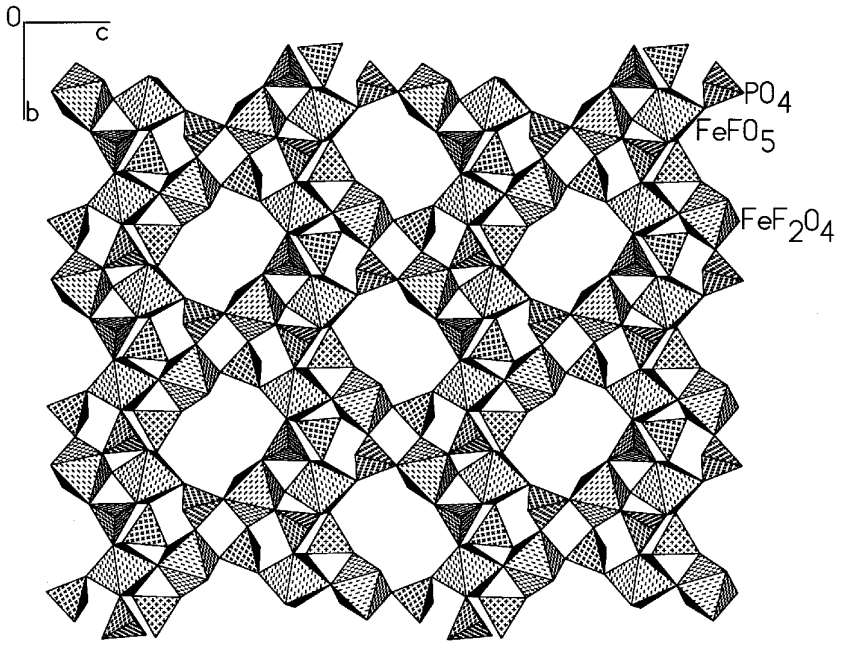

Figure 3. The polyhedral view of the structure of **I** $[C_6N_4H_{21}][Fe_2F_2(HPO_4)_3][H_2PO_4]\cdot 2H_2O$ along the *bc* plane showing the 3-, 4- and 8-membered rings.

Table 4. Selected bond angles in **I** $[C_6N_4H_{21}][Fe_2F_2(HPO_4)_3][H_2PO_4]\cdot 2H_2O$.

Moiety	Angle (°)	Moiety	Angle (°)
F(1)–Fe(1)–O(1)	90·81(11)	O(7)$^{\#1}$–P(1)–O(2)	111·83(14)
F(1)–Fe(1)–O(2)	176·63(10)	O(5)–P(1)–O(10)	108·7(2)
O(1)–Fe(1)–O(2)	92·12(11)	O(7)$^{\#1}$–P(1)–O(10)	103·59(14)
F(1)–Fe(1)–F(2)	89·48(9)	O(2)–P(1)–O(10)	106·04(14)
O(1)–Fe(1)–F(2)	87·61(10)	O(9)–P(2)–O(8)$^{\#2}$	113·4(2)
O(2)–Fe(1)–F(2)	88·98(9)	O(9)–P(2)–O(3)	112·64(14)
F(1)–Fe(1)–O(3)	87·27(10)	O(8)$^{\#2}$–P(2)–O(3)	111·2(2)
O(1)–Fe(1)–O(3)	176·68(12)	O(9)–P(2)–O(11)	107·9(2)
O(2)–Fe(1)–O(3)	89·73(10)	O(8)$^{\#2}$–P(2)–O(11)	101·3(2)
F(2)–Fe(1)–O(3)	89·67(10)	O(3)–P(2)–O(11)	109·6(2)
F(1)–Fe(1)–O(4)	92·00(10)	O(1)$^{\#3}$–P(3)–O(4)	113·3(2)
O(1)–Fe(1)–O(4)	89·82(11)	O(1)$^{\#3}$–P(3)–O(6)$^{\#4}$	111·5(2)
O(2)–Fe(1)–O(4)	89·67(10)	O(4)–P(3)–O(6)$^{\#4}$	111·34(14)
F(2)–Fe(1)–O(4)	177·05(10)	O(1)$^{\#3}$–P(3)–O(12)	109·5(2)
O(3)–Fe(1)–O(4)	92·95(10)	O(4)–P(3)–O(12)	103·94(14)
F(2)–Fe(2)–O(5)	91·30(10)	O(6)$^{\#4}$–P(3)–O(12)	106·7(2)
F(2)–Fe(2)–O(6)	177·16(10)	O(13)–P(4)–O(14)	114·4(2)
O(5)–Fe(2)–O(6)	88·75(10)	O(13)–P(4)–O(15)	113·0(2)
F(2)–Fe(2)–O(7)	89·12(10)	O(14)–P(4)–O(15)	106·7(2)
O(5)–Fe(2)–O(7)	175·14(11)	O(13)–P(4)–O(16)	109·1(3)
O(6)–Fe(2)–O(7)	91·07(10)	O(14)–P(4)–O(16)	105·8(2)
F(2)–Fe(2)–O(8)	90·15(10)	O(15)–P(4)–O(16)	107·4(2)
O(5)–Fe(2)–O(8)	90·42(10)	P(3)$^{\#3}$–O(1)–Fe(1)	170·5(2)
O(6)–Fe(2)–O(8)	92·69(10)	Fe(2)–F(2)–Fe(1)	133·67(11)
O(7)–Fe(2)–O(8)	84·73(10)	P(1)–O(2)–Fe(1)	133·3(2)
F(2)–Fe(2)–O(9)	86·73(9)	P(2)–O(3)–Fe(1)	131·7(2)
O(5)–Fe(2)–O(9)	91·20(10)	P(3)–O(4)–Fe(1)	128·9(2)
O(6)–Fe(2)–O(9)	90·43(10)	P(1)–O(5)–Fe(2)	132·5(2)
O(7)–Fe(2)–O(9)	93·66(10)	P(3)$^{\#5}$–O(6)–Fe(2)	131·3(2)
O(8)–Fe(2)–O(9)	176·52(10)	P(1)$^{\#2}$–O(7)–Fe(2)	146·4(2)
O(5)–P(1)–O(7)$^{\#1}$	112·8(2)	P(2)$^{\#1}$–O(8)–Fe(2)	140·0(2)
O(5)–P(1)–O(2)	113·13(14)	P(2)–O(9)–Fe(2)	142·4(2)
Organic moiety			
C(5)–N(1)–C(3)	113·2(3)	N(2)–C(2)–C(1)	112·6(4)
C(5)–N(1)–C(1)	111·6(3)	N(1)–C(3)–C(4)	111·9(3)
C(3)–N(1)–C(1)	112·3(3)	N(3)–C(4)–C(3)	112·5(3)
N(1)–C(1)–C(2)	108·6(4)	N(1)–C(5)–C(6)	112·3(4)
		N(4)–C(6)–C(5)	112·2(4)

Symmetry transformations used to generate equivalent atoms: $^{\#1}-x, y-1/2, -z+3/2$; $^{\#2}-x, y+1/2, -z+3/2$; $^{\#3}-x, -y, -z+1$; $^{\#4}x, -y+1/2, z-1/2$; $^{\#5}x, -y+1/2, z+1/2$

There are two crystallographically distinct Fe atoms and four distinct P atoms in the asymmetric unit. The Fe(1) and Fe(2) atoms in **I** make 4 and 5 Fe–O–P bonds with their three distinct P neighbors respectively, and also share a bridging F between them via a Fe(1)–μF(2)–Fe(2) linkage to form a $Fe_2F_2O_9$ dimer. The sixth coordination needed to satisfy the octahedral coordination of Fe(1) comes from a terminal F-atom. The presence of terminal fluorine is not uncommon and has been observed in FePO[4], AlPO[34–36] and GaPO[37]. The Fe–O bond distances in **I** are in the range 1·953(3) Å–2·0493 Å [$(Fe(1)–O)_{av}$ = 1·9885; $(Fe(2)–O)_{av}$ = 1·9962]. The *trans* O/F–Fe–O bond angles are in the range

175·14(11)°–177·16(10)° [$(O/F–Fe(1)–O)_{av}$ = 176·7866°; $(O/F–Fe(2)–O)_{av}$ = 176·2733], and *cis* F/O–Fe–O angles are in the range 84.73(10)° – 93.66(10)° [$(O/F–Fe(1)–O)_{av}$ = 90·01; $(O/F–Fe(2)–O)_{av}$ = 90·0208]. The four distinct P atoms in **I** are tetrahedrally coordinated by oxygens. Out of the four, 3 P atoms [P(1), P(2), P(3)] make 3 P–O–Fe bonds with two different Fe atoms and the remaining P–O vertex being terminal. On the other hand P(4) has all the four oxygens as terminal. The P–O distances are in the range 1·482(3) Å – 1·588(3) Å [$(P(1)–O)_{av}$ = 1·5332 Å; $(P(2)–O)_{av}$ = 1·5357Å; $(P(3)–O)_{av}$ = 1·5312 Å; $(P(4)–O)_{av}$ = 1·5172]. The O–P–O bond angles are in the range 101·3(2)° – 114·4(2)° [$(O–P(1)–O)_{av}$ = 109·35 Å; $(O–P(2)–O)_{av}$ = 109·34 Å; $(O–P(3)–O)_{av}$ = 109·38 Å and $(O–P(4)–O)_{av}$ = 109·40 Å]. Of the eighteen O atoms, 9 form Fe–O–P linkages between two Fe and three P atoms (P(1), P(2), P(3)), with Fe–O–P bond angles in the range 128·9(2)° – 170·5(2)°. Seven oxygens form terminal P–O bond while the

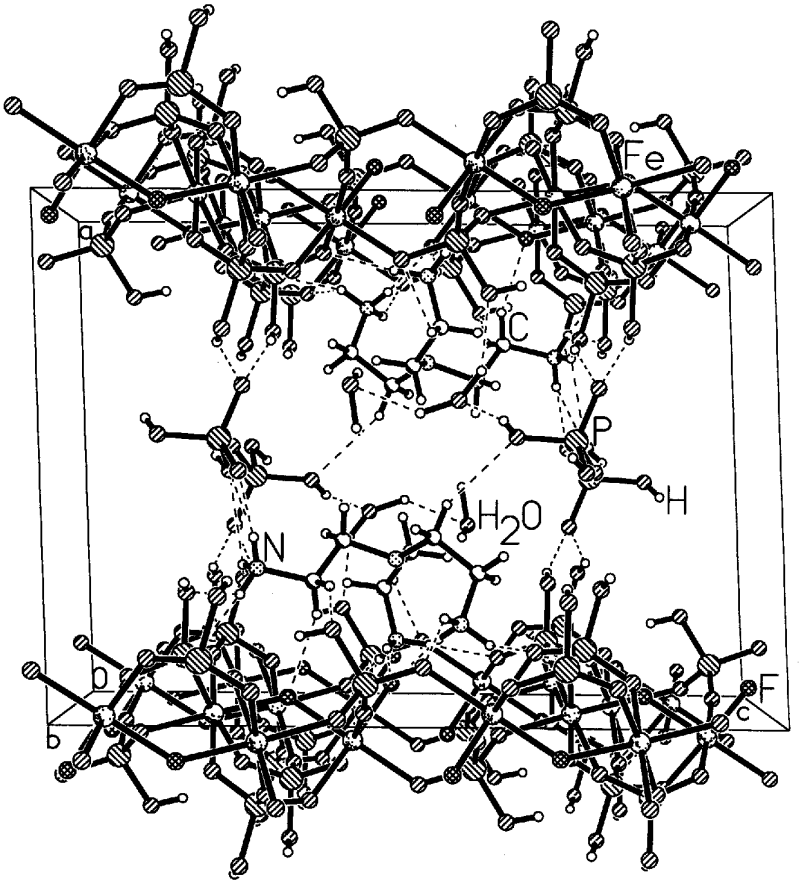

Figure 4. Structure of **I** $[C_6N_4H_{21}][Fe_2F_2(HPO_4)_3][H_2PO_4]·2H_2O$ along the *b*-axis. Amine, $H_2PO_4^-$ and water molecules occupy the interlayer space. Dotted lines represent hydrogen bond interactions.

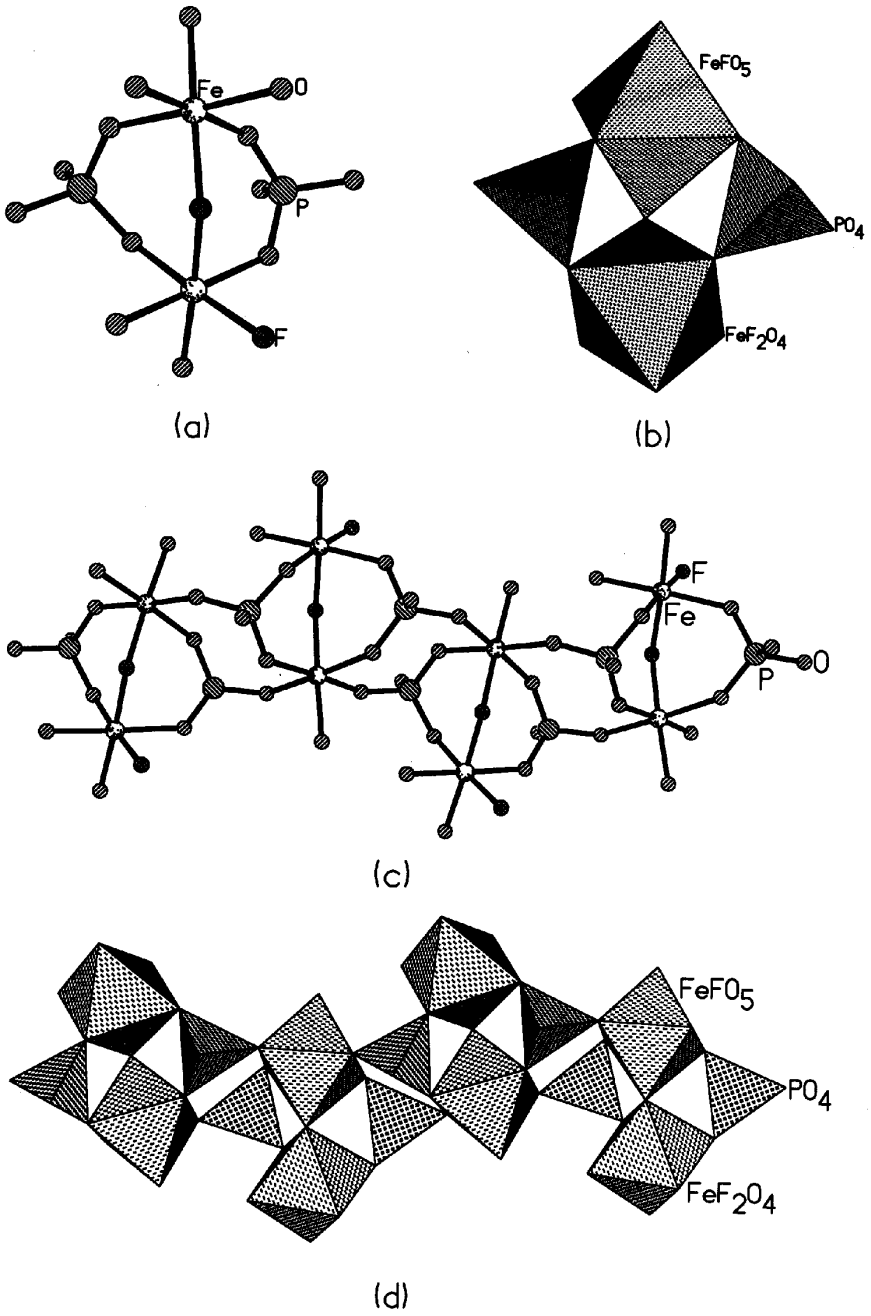

Figure 5. (**a**) and (**b**) Figures showing the secondary building unit of **I** $[C_6N_4H_{21}][Fe_2F_2(HPO_4)_3][H_2PO_4]\cdot 2H_2O$. Note that two HPO_4 groups cap the $Fe_2F_2O_9$ dimer. (**c**) and (**d**) Chains formed by the joining of the SBUs. Note that the two chains run parallel but in opposite direction along the *b*-axis.

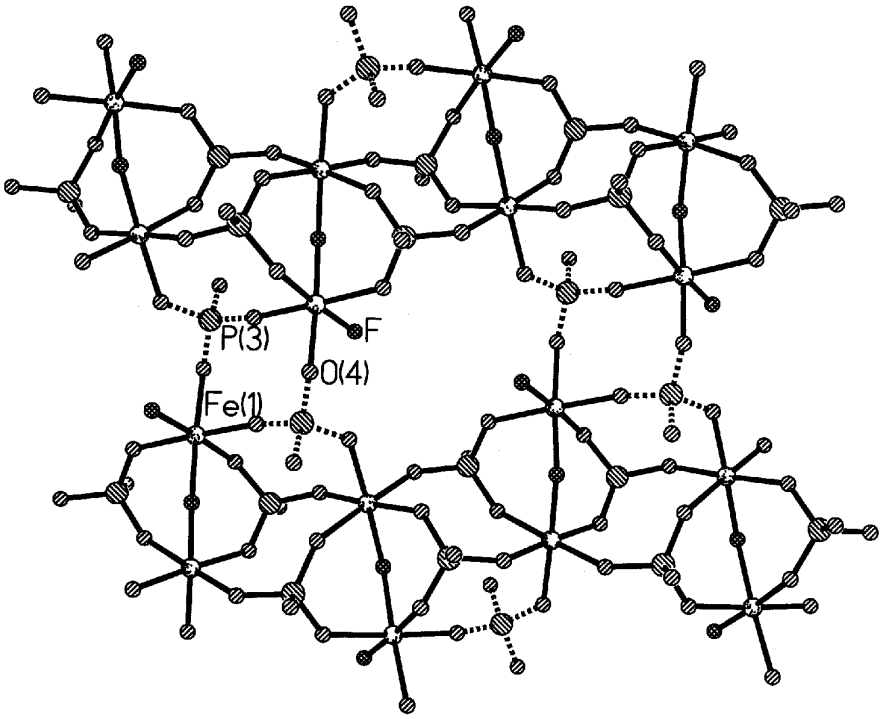

Figure 6. The joining of the two chains by the $HP(3)O_4$ group has been shown. Fe–O–P connectivity has been shown as dotted lines.

remaining two oxygens [O(100) and O(200)] are from the free water molecules. Amongst the seven terminal O, five are formally terminal –OH groups [P(1)–O(10) = 1·577(3) Å; P(2)–O(11) = 1·574(3) Å; P(3)–O(12) = 1·588(3) Å; P(4)–O(15) = 1·538(3) Å and P(4)–O(16) = 1·554(3) Å]. The remaining two are terminal P = O groups [P(4)–O(13) = 1·482(3) Å; P(4)–O(14) = 1·495(3) Å]. The proton positions corresponding to the terminal P–O moiety were observed in difference Fourier map. The observed P–OH bond lengths are in agreement with the standard literature values for the terminal hydroxyl groups, such as $H_3PO_4 – 0·5H_2O$ and α-zirconium phosphate with distances of 1·551 and 1·558 Å respectively[38]. This assignment of proton position is consistent with the bond valence sum calculations (O(10) = 1·1124, O(11) = 1·1232, O(12) = 1·0815, O(15) = 1·2380 and O(16) = 1·1856)[39]. Detailed bond valence sum calculations (P(1) = 5·0277, P(2) = 4·9908, P(3) = 5·0657, P(4) = 5·2545, Fe(1) = 3·1263 and Fe(2) = 3·1146) also indicated that the valence state of the Fe and P are +3 and +5 respectively. So the framework stoichiometry of $[Fe_2F_2(HPO_4)]^{2-}$ along with the free $[H_2PO_4]^-$ produces a charge of −3 which thus directs that all the three terminal $–NH_2$ groups of the *tris*-(2-aminoethylamine) are protonated. This is in agreement with the final formula of $[C_6N_4H_{21}][Fe_2F_2(HPO_4)_3][H_2PO_4]·2H_2O$.

The topology of the layer in **I** can be described in terms of a secondary building unit (SBU). It has been mentioned earlier that FeF_2O_4 and $FeFO_5$ octahedra are corner-shared

by Fe(1)-μF(2)-Fe(2) bond to form a $Fe_2F_2O_9$ dimer. The SBU is constructed from the capping of the dimer by two HPO_4 groups ($HP(1)O_4$ and $HP(2)O_4$) as shown in figures 5(a) and (b) and the capping creates two 3-membered rings in the SBU. Such tetrameric (M_2P_2) SBUs have been described as SBU-4 by Férey[40] and observed earlier in AlPO[35,36] and GaPO[37,41] systems. The SBUs are connected to each other through a 4-membered ring involving corner-sharing Fe–O–P linkages, thereby forms a sinusoidal chain as shown in figures 5(c) and (d). In the layer such chains run parallel along *b*-direction and are covalently connected to each other by the $HP(3)O_4$ group. The $HP(3)O_4$ group connects the chains via three Fe–O–P linkages as shown in figure 6. Such linkages also create two 4-membered rings and an 8-membered ring of width $5{\cdot}531 \times 10{\cdot}596$ Å (nearest O–O contacts not including the van der Waals radii) within the layer (figure 6). So the three phosphate groups in the layer coordinate to the Fe-centers through three oxygen donors, the fourth oxygen is present as pendant P–OH group projecting into the interlamellar space and interacting strongly with the protonated amine, intercalated $H_2PO_4^-$ and H_2O (figure 4).

The structure is stabilized by extensive hydrogen bonding. The tripodal amine interacts with the inorganic layer through strong N–H…O hydrogen bonding and caps the 8-membered aperture from top and bottom like the talons of a claw. There appear to be weak N–H…F bonding involving the terminal fluorine of inorganic layer. The layers are held ~13 Å apart not because of the amine alone. The intercalated $H_2PO_4^-$ groups interact strongly through hydrogen bonding with the inorganic layers as well as with the amines, and play the role of pillaring the layers (figure 7). Such pillaring by free $H_2PO_4^-$ in open-framework solids has been observed for the first time. Details of hydrogen bonding interactions are listed in the table 5.

Table 5. Selected hydrogen bond interactions in **I** $[C_6N_4H_{21}][Fe_2F_2(HPO_4)_3][H_2PO_4]{\cdot}2H_2O$.

Moiety	Distance (Å)	Moiety	Angle (°)
O(11)…H(5)	2·466(4)	O(11)…H(5)–N(2)	130·2(4)
O(8)…H(5)	2·171(5)	O(8)…H(5)–N(2)	163·4(3)
O(10)…H(6)	2·066(4)	O(10)…H(6)–N(2)	151·8(4)
O(14)…H(7)	1·880(5)	O(14)…H(7)–N(2)	170·5(4)
O(6)…H(12)	2·029(4)	O(6)…H(12)–N(3)	164.4(4)
F(1)…H(13)	1·858(4)	F(1)…H(13)–N(3)	156·5(4)
O(3)…H(14)	2·040(4)	O(3)…H(14)–N(3)	163·1(3)
O(7)…H(19)	2·073(4)	O(7)…H(19)–N(2)	163·4(3)
O(10)…H(6)	2·066(4)	O(10)…H(6)–N(4)	153·6(4)
F(1)…H(20)	1.830(5)	F(1)…H(20)–N(4)	162·6(4)
O(4)…H(21)	2·512(5)	O(4)…H(21)–N(4)	140·7(4)
O(13)…H(22)	1·833(4)	O(13)…H(22)–O(10)	147·8(3)
O(13)…H(23)	1·886(4)	O(13)…H(23)–O(11)	148·4(4)
O(9)…H(24)[1]	1·946(4)	O(9)…H(24)–O(12)	145·3(3)
O(14)…H(25)	1·857(5)	O(14)…H(25)–O(15)	137·0(5)
O(100)…H(26)	1·850(7)	O(100)…H(26)–O(16)	162·7(6)
O(12)…H(27)	2·000(2)	O(12)…H(27)–O(100)	143·0(17)
F(2)…H(3)	2·333(6)	F(2)…H(3)–C(2)	129·8(5)
O(12)…H(4)	2·508(6)	O(12)…H(4)–C(2)	151·7(4)
O(4)…H(11)	2·572(5)	O(4)…H(11)–C(4)	125·2(4)
O(16)…H(16)	2·573(5)	O(16)…H(16)–C(5)	152·6(5)

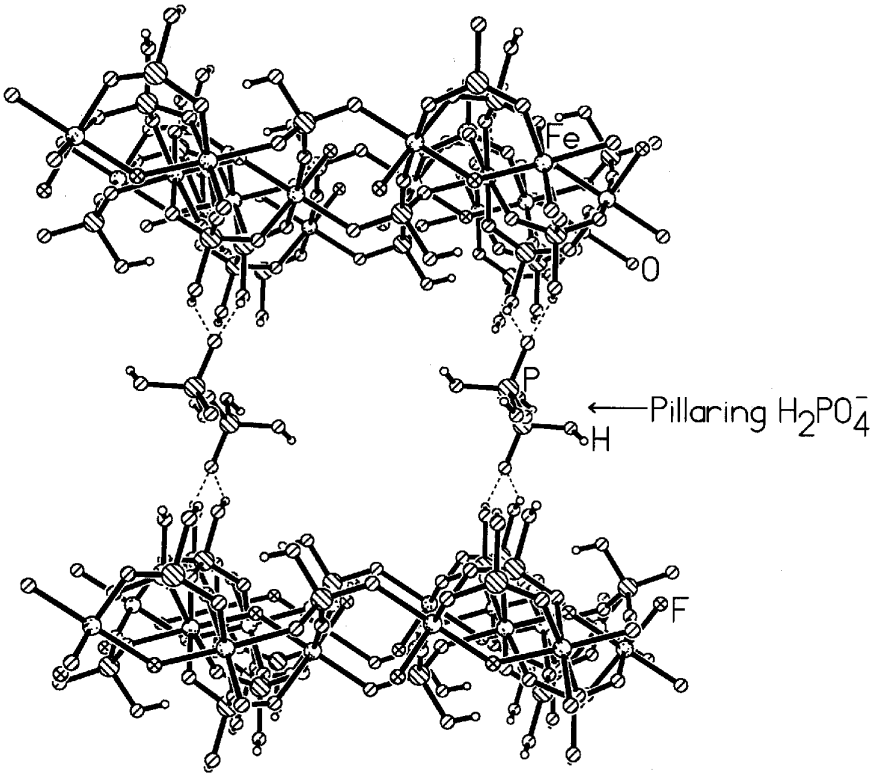

Figure 7. The pillaring role of the intercalated $H_2PO_4^-$ has been shown. Dotted lines represent hydrogen bond interactions.

Thermogravimetric analysis (TGA) of **I** reveals that there are two major steps of weight loss, centered around 100°C and 350°C as shown in figure 8. The first step corresponds to the loss of two H_2O molecule (obs. – 4·6453%, calc. – 5·00%), while the second step which has a sharp jump at 300°C followed by a long tail corresponds to the loss of amine molecule, HF, and a phosphoryl – OH group (obs – 37·8%, calc – 31·33%). The final calcined product at 850°C is dense $Fe(PO_3)_2$ [JCPDS file card no. 30-0660].

4. Conclusions

The layer topology in **I** is new although many open-framework iron phosphates have their structural analogs in the GaPO[11,12,19,20] and AlPO systems[10,42] or in the naturally occurring iron phosphate mineral[43]. The presence of Fe–O/F–Fe linkage is common in open-framework iron phosphate and also in mineral but the diversity lies in their connectivity. The Fe–O/F–Fe connectivity leads to infinite chains of vertex[6,8,10,21] or edge-sharing[11,12,14] FeF_xO_{6-x} (x = 0–2) octahedra, finite chains e.g. a pentamer[5], or a trimer which is found in all SBU-6[18–20] and even some unusual clusters[7,13,22,25]. Iron Phosphate framework exclusively built up from isolated iron octahedra surrounded by

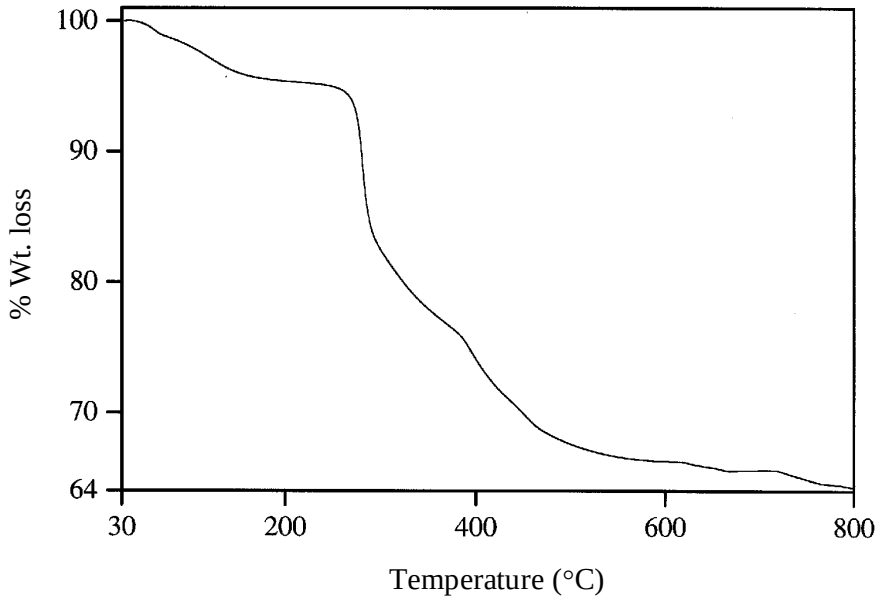

Figure 8. TGA curve for $[C_6N_4H_{21}][Fe_2F_2(HPO_4)_3][H_2PO_4]\cdot 2H_2O$ (**I**).

phosphate groups is very rare[16,17,24,28]. On the other hand, structures formed exclusively from the isolated corner-shared iron octahedral dimer surrounded by phosphate groups have been observed for the first time. Pillaring of iron phosphate layers by free $H_2PO_4^-$ groups is unique and has not been observed earlier in open-framework structures, though the pillaring of iron phosphate layers by phosphate groups through covalent bonds is known[4].

The synthetic procedure of the iron phosphate merits some discussion. Encouraged by our earlier investigations[5] we have used $Fe(acac)_3$ as the source of iron along with different amines. Use of the same molar ratio of the reactants does not lead to the same structure if the iron source is different (e.g. $FeCl_3$ or Fe_2O_3). $Fe(acac)_3$ as a precursor for the iron phosphate provides a new strategy for the synthesis of novel open framework iron phosphates besides the other two already existing routes[2,3].

Acknowledgements

The author thanks Prof. C N R Rao, FRS, for discussions, support and encouragement. The author also thanks the Council of Scientific and Industrial Research (CSIR), Government of India, for a fellowship.

References

1. Cheetham A K, Loiseau T and Ferey G 1999 *Angew. Chem., Int. Ed. Engl.* **38** 3268
2. Lii K H, Huang Y F, Zima V, Huang C Y, Lin H M, Jiang Y C, Liao F L and Wang S L 1998 *Chem. Mater.* **10** 2599

3. Cavellec M, Riou D and Férey G 1999 *Inorg. Chim. Acta.* **291** 317
4. Choudhury A, Natarajan S and Rao C N R 1999 *Chem. Commun.* 1305
5. Choudhury A and Natarajan S 2000 *J. Solid State Chem.* **154** 507
6. Cavellec M, Riou D, Grenèche J-M and Férey G 1997 *Inorg. Chem.* **36** 2187
7. Zima V and Lii K H 1998 *J. Chem. Soc., Dalton Trans.* 4109
8. Lethbridge Z A D, Lightfoot P, Morris R E, Wragg D S, Wright P A, Kvick Å and Vaughnan G 1999 *J. Solid State Chem.* **142** 455
9. Cavellec M, Riou D and Ferey G 1994 *J. Solid State Chem.* **112** 441
10. Cavellec M, Riou D and Ferey G 1995 *Eur. J. Solid State Chem.* **32** 271
11. Cavellec M, Riou D and Ferey G 1995 *Acta. Crystallogr.* **C51** 2242
12. DeBord J R D, Reiff W M, Haushalter R C and Zubieta J 1996 *J. Solid State Chem.* **125** 186
13. Lii K H and Huang Y F 1997 *Chem. Commun.* 1311
14. Zima V, Lii K H, Nguyen N and Ducouret A 1998 *Chem. Mater.* **10** 1914
15. Cavellec M R, Greeneche J M, Riou D and Ferey G 1998 *Chem. Mater.* **10** 2434
16. Mgaidi A, Boughzala H, Driss A, Clerac R and Coulon C 1999 *J. Solid State Chem.* **144** 163
17. Cowley A R and Chipendale A M 2000 *J. Chem. Soc., Dalton Trans.* 3425
18. Cavellec M, Riou D, Ninclaus C, Grenèche J M and Férey G 1996 *Zeolites* **17** 250
19. Cavellec M, Riou D, Grenèche J M and Férey G 1996 *J. Magn. Magn. Mater.* **163** 173
20. Cavellec M, Egger C, Linares J, Nogues M, Varret F and Férey G 1997 *J. Solid State Chem.* **134** 349
21. Cavellec M, Grenèche J M, Riou D and Férey G 1997 *Microporous Mater.* **8** 103
22. DeBord J R D, Reiff W M, Warren C J, Houshalter R C and Zubieta J 1997 *Chem. Mater.* **9** 1994
23. Lii K H and Huang Y F 1997 *Chem. Commun.* 839
24. Lii K H and Huang Y F 1997 *J. Chem. Soc., Dalton Trans.* 2221
25. Huans C Y, Wang S L and Lii K H 1998 *J. Porous Mater.* **5** 147
26. Cavellec M, Grenèche J M and Férey G 1998 *Microporous Mesoporous Mater.* **20** 45
27. Zima V and Lii K H 1998 *J. Solid State Chem.* **139** 326
28. Choudhury A and Natarajan S 2000 *Int. J. Inorg. Mater.* **2** 217
29. Chaudhuri M K and Ghosh S 1983 *J. Chem. Soc., Dalton Trans.* 839
30. Vogel A I 1989 *Textbook of quantitative chemical analysis* 5th edn (Edinburg Gate: Addison Wesley–Longman)
31. Sheldrick G M 1994 *SADABS Siemens area detector absorption correction program* (Germany: University of Göttingen)
32. Sheldrick G M 1986 *SHELXS-86 Program for crystal structure determination* (University of Göttingen); Sheldrick G M 1990 *Acta Crystallogr.* **A35** 467
33. Sheldrick G M 1993 *SHELXTL-PLUS Program for crystal structure solution and refinement* (Germany: University of Götingen)
34. Yu L, Pang W and Li L 1990 *J. Solid State Chem.* **87** 241
35. Taulelle F, Loiseau T, Maquet J, Livage J and Féray G 1993 *J. Solid State Chem.* **105** 191
36. Yan W, Yu J, Shi Z and Xu R 2001 *Inorg. Chem.* **40** 379
37. Férey G, Loiseau T, Laccore P and Taulelle F 1993 *J. Solid State Chem.* **105** 179
38. Troup J M and Clearfield A 1977 *Inorg. Chem.* **16** 3311
39. Brown I D and Altermatt D 1984 *Acta Crystallogr.* **B41** 244
40. Férey G 1995 *J. Fluorine Chem.* **72** 187
41. Loiseau T and Férey G 1992 *J. Chem. Soc., Chem. Commun.* 1179
42. Riou D, Losieau T and Férey G 1993 *J. Solid State Chem.* **102** 4
43. Cavellec M, Riou D and Férey G 1994 *Acta Crystallogr.* **C50** 1379